JACS
JOURNAL OF THE AMERICAN CHEMICAL SOCIETY
Article
pubs.acs.org/JACS

Understanding the Role of Defect Sites in Glucan Hydrolysis on Surfaces

Oz M. Gazit and Alexander Katz*

Department of Chemical and Biomolecular Engineering, University of California, Berkeley, California, United States

Supporting Information

ABSTRACT: Though unfunctionalized mesoporous carbon consisting of weakly Brønsted acidic OH-defect sites depolymerizes cellulose under mild conditions, the nature of the active site and how this affects hydrolysis kinetics—the rate-limiting step of this process—has remained a puzzle. Here, in this manuscript, we quantify the effect of surface OH-defect site density during hydrolysis catalysis on the rate of reaction. Our comparative approach relies on synthesis and characterization of grafted poly(1→4-β-glucan) (β-glu) strands on alumina. Grafted β-glu strands on alumina have a 9-fold higher hydrolysis rate per glucan relative to the highest rate measured for β-glu strands on silica. This amounts to a hydrolysis rate per grafted center on alumina that is 2.7-fold more active than on silica. These data are supported by the lower measured activation energy for hydrolysis of grafted β-glu strands on alumina being 70 kJ/mol relative to 87 kJ/mol on silica. The observed linear increase of hydrolysis rate with increasing OH-defect site density during catalysis suggests that the formation of hydrogen bonds between weakly Brønsted acidic OH-defect sites and constrained glycosidic oxygens (i.e., those juxtaposed adjacent to the surface) activates the latter for hydrolysis catalysis. Altogether, these data elucidate crucial structural requirements for glucan hydrolysis on surfaces and, when coupled with our recent demonstration of long-chain glucan binding to mesoporous carbon, present a unified picture, for the first time, of adsorbed glucan hydrolysis on OH-defect site-containing surfaces, such as unfunctionalized mesoporous carbon.

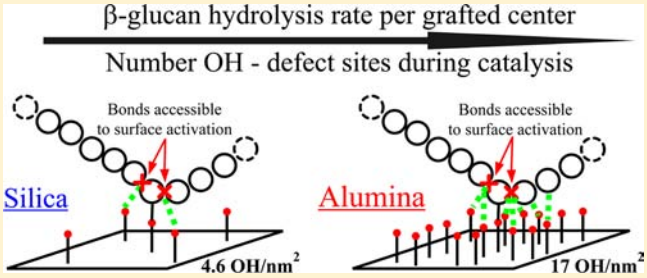

INTRODUCTION

Understanding essential features of weak Brønsted acid catalysts for cellulose hydrolysis, such as unfunctionalized mesoporous carbon, is invaluable to the rational design and implementation of new catalysts for biomass depolymerization,[1] which due to their mild surface acidity, should be able to function in the presence of salt prevalent in biomass without leaching acid sites via exchange processes. While we have recently demonstrated that long-chain glucans will readily and rapidly (faster than the time scale of sampling in experiments) adsorb to internal pores of mesoporous carbon, even though they have significantly larger hydrodynamic diameters than the mesopores of the carbon,[2] the hydrolysis of these constrained glucans remains a challenge and a subject of intense ongoing efforts.[3,4] Enzymes such as cellulase and lysozyme serve as a paradigm for the development of synthetic cellulose hydrolysis catalysts that function at mild pH and temperature.[5,6] An essential feature of the enzyme active site consists of a carboxylic acid hydrogen bond donor to the glycosidic oxygen, which activates it for hydrolysis by improving leaving group ability within the hydrolysis transition state.[5,7−10] Results from pioneering intramolecular catalysis studies emphasize the importance of rigid juxtapositioning and high local density of such a carboxylic acid donor adjacent to the glycosidic oxygen[11,12] in order to catalyze hydrolysis.[10,13] Recently, with these paradigms in mind, we demonstrated hydrolysis of grafted poly(1→4-β-glucan) (β-glu) strands on silica, according to a hypothesized mechanism of the inorganic oxide surface acting as a catalyst. While surface OH-defect sites have been previously used as catalysts in the gas phase and organic solvents,[14,15] there is no proof of their catalytic activity in water.

In this contribution, we present strong evidence of OH-defect site catalysis in water by quantitatively investigating the effect of OH-defect site density during catalysis. This was not possible previously because all grafted β-glu materials investigated previously were on a silica support, and consequently, they all possessed the same OH-defect site density during hydrolysis catalysis, which is limited by the maximum OH density on silica. In this contribution, a comparative study including grafted β-glu strands on alumina permits investigation of the effect on the reaction kinetics of OH-defect site density during hydrolysis. Quantitative results demonstrate that this density controls hydrolysis catalysis of glucans on surfaces via hydrogen-bond formation between OH-defect sites and glycosidic oxygens that are constrained due to surface adsorption.

Received: December 6, 2012
Published: February 15, 2013

dx.doi.org/10.1021/ja311918z | J. Am. Chem. Soc. 2013, 135, 4398−4402

RESULTS AND DISCUSSION

Our approach builds on a comparative study of materials represented in Scheme 1, consisting of submonolayer coverages of grafted β-glu strands within a hydrogen-bonding environment that is controlled by OH-defect sites on the surrounding metal-oxide surface.

Scheme 1. Schematic Description of Adsorbed β-Glu Strands on the Metal Oxide Surface[a]

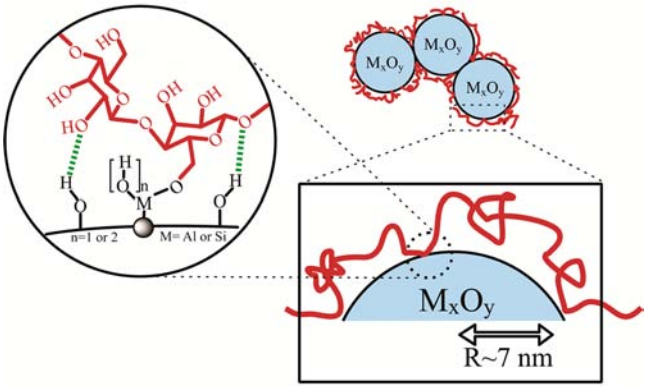

[a]These strands consist of loops and grafted sites on the surface. The size of the loops and grafted-site density on the surface is controlled by the OH-defect site density during grafting.

Within the context of this scheme, a grafted active site refers to the site where covalent M−O−glucan contact is made between a cellobiose repeat unit of the β-glu strands and the underlying inorganic-oxide surface. The synthesis of these materials entails activating OH-defect sites on the surface for grafting of strands from dilute solution via reaction with M−X, where X represents a good leaving group (e.g., X = Cl for M = Si and X = CH_3 for M = Al). We previously demonstrated, for silica-based materials, that the OH-defect site density during β-glu grafting controls the density of grafted active sites.[16] This is manifested in the observed increase of the combustion temperature of the grafted β-glu strands upon increasing the density of OH-defect sites during grafting (see Figure 1S in Supporting Information [SI]). This increase arises due to differences in the OH-defect site density during, rather than after, β-glu grafting, since all materials were extensively washed with water for a period of 24 h and therefore have the same density of surface hydroxyls prior to thermogravimetric analysis.

The increase in hydrolysis reaction rates, as measured in aqueous solution at 95 °C and pH 4, upon increasing OH-density during grafting is shown in Figure 1 for various grafted β-glu materials. These data show that the rate of grafted β-glu strand hydrolysis on silica increases linearly with density of silanol OH-defect sites that are present during grafting. The scaling shown in Figure 1 for the silica-based materials (lowest OH-density during grafting on silica (SGEXL), low OH-density during grafting on silica (SGL), and high OH-density during grafting on silica (SGH)) equates a grafted active site to the active site where catalyzsis occurs; however, it does not elucidate which structural features of the active site lead to hydrolysis catalysis under such mild conditions of surface acidity and temperature. It is important to emphasize that the number of OH-defect sites during hydrolysis in aqueous solution is the same in all silica-based materials in Figure 1, because a silica under aqueous reaction conditions consists of a fully hydroxylated surface at a maximum silanol density of 4.6 OH/nm^2.[17]

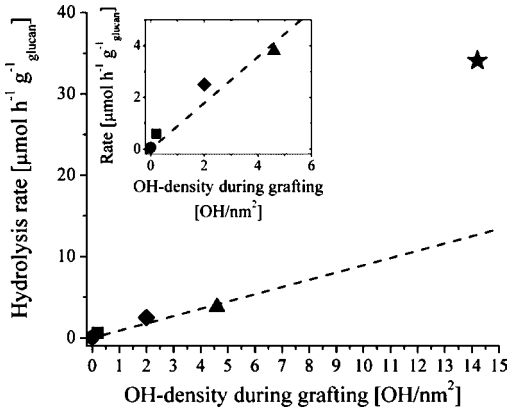

Figure 1. Rate of grafted β-glu strand hydrolysis increases with density of OH-defect sites during β-glu grafting. Hydrolysis reaction conducted at 95 °C and pH 4 aqueous solution: (●) Amorphous cellulose. (■) Lowest OH-density during grafting on silica (SGEXL). (♦) Low OH-density during grafting on silica (SGL). (▲) High OH-density during grafting on silica (SGH). (★) Low OH-density during grafting on alumina (AGL). Rates for hydrolysis at 95 °C (corresponding to oil bath temperature of 105 °C) corresponding to those for amorphous cellulose, SGEXL, and SGL are taken from ref 16. OH-defect site densities are obtained using TGA and are consistent with previous reports for pretreated silica and alumina.

Investigation of the effect of OH-defect site density that is present during hydrolysis catalysis on reaction kinetics requires varying this density by changing the support. We chose to compare hydrolysis of grafted β-glu on silica and alumina supports because the number density of OH-defect sites for silica and alumina surfaces during aqueous reaction conditions is expected to be significantly different. Alumina has a monolayer OH-defect site density of up to 17 OH/nm^2,[18,19] corresponding to an average distance between defect sites of 2.4 Å, which is nearly half of the distance for silica, which is 4.7 Å. However, the acidity of the defect sites on alumina and silica is expected to be similar. The similarity of the acidity of OH-defect sites between the silica and alumina materials is manifested by the fact that a slurry of the alumina creates a pH of 5.6 in water, whereas a similar slurry of silica leads to a pH of 4.9, both of which are significantly higher than the aqueous-phase pH of 4.0 used in hydrolysis reactions here (see SI). The use of weak-acid sites, such as OH-defect sites on alumina and silica, prevents any significant dissociation to form surface conjugate base anions during hydrolysis catalysis. The formation of such anions and delocalized hydrated protons would not be expected to activate the glycosidic oxygen for hydrolysis reaction due to the lack of hydrogen-bond donors. The latter would only be capable of low reactivity under a specific acid-catalyzed mechanism, under the mild reaction conditions investigated here. This is supported by data for the physical mixture of silica and reprecipitated and ball-milled cellulose control in Figure 1.[16]

The approach for synthesizing the required grafted β-glu strands on alumina material (AGL) is shown in Figure 2. Fumed alumina (Aeroxide Alu C, 100 m^2/g, primary particle size of ~13 nm) is used as a support for β-glu grafting without pretreatment, at a surface hydroxyl density of 14.2 OH/nm^2 according to thermal gravimetric analysis (TGA) (see Figure 2S in SI). The synthetic procedure for grafting on the alumina

dx.doi.org/10.1021/ja311918z | J. Am. Chem. Soc. 2013, 135, 4398−4402

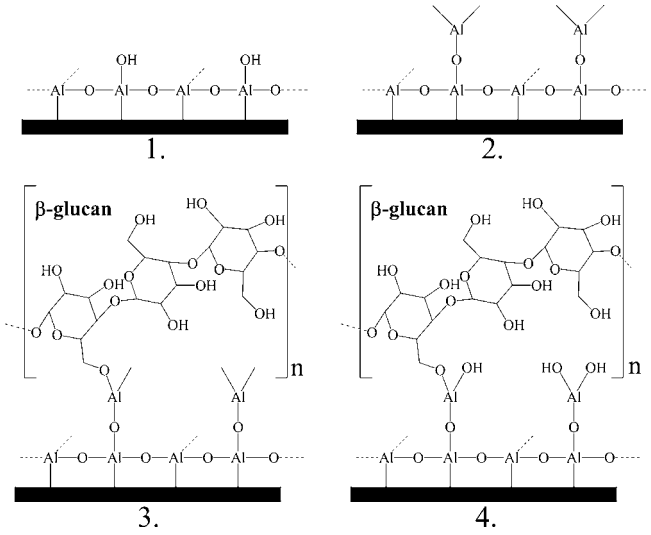

Figure 2. Schematic representation of the grafting procedure of β-glu strands on the surface of alumina: (1) dry alumina, (2) TMA-treated alumina, (3) grafting of β-glu, and (4) extensive washing and drying.

surface is discussed below.[16] Alumina is activated for grafting by using trimethylaluminum (TMA) in order to keep the composition of the system consistent with alumina rather than a significantly more Brønsted acidic aluminosilicate. The addition of dry, dilute β-glu solution and rigorous washing and drying of the material follow a procedure similar to what was performed in the synthesis of the silica-based systems.

TGA of grafted β-glu strands on alumina (represented by the AGL material) show a mass loading of 1.6 wt % β-glu relative to alumina (see inset in Figure 3). The packing fraction of the grafted β-glu strands in AGL is calculated to be 0.22 (see Table 1), which is well below the 0.65 jamming limit for random sequential adsorption of polymers.[20,21] Solid-state ^{13}C CP/MAS NMR data shown in Figure 3 clearly show the absence of the two distinct resonances at 89 and 65 ppm that represent crystalline cellulose.[22] These data indicate that, as in the case of

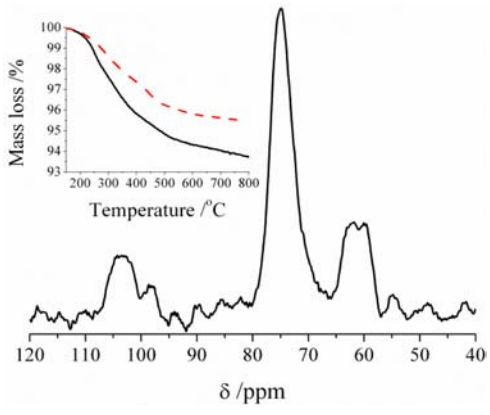

Figure 3. ^{13}C CP/MAS solid-state NMR of β-glu strands grafted on alumina material AGL. Spectrum shows the absence of the resonances at 89 ppm and 65 ppm that correspond to crystalline cellulose.[22] This data indicates that the grafted β-glu strands on alumina have an amorphous-like structure. Inset: TGA of glucan grafted alumina (black solid line). Red dotted line represents control material that has seen the full synthesis procedure, except with glucan being absent from the grafting solution. TGA shows that the glucan amount on the alumina support is 1.6% or 16 mg/g alumina support.

the silica-based system, the grafted β-glu strands on AGL are amorphous in nature and likely interact with nearby surface OH-defect sites (aluminols), rather than with other β-glu strands.

Hydrolysis of grafted β-glu strands on silica and alumina was conducted under mild conditions of pH 4 HCl in aqueous solution at 358 − 388 K (autogenous pressure). The number of hydrolytic events occurring during the course of the reaction was measured using a 2,2′-bicinchoninate (BCA) colorimetric method, which monitors the concentration of reducing ends per mass of β-glu strand.[16] As demonstrated by data in Figure 3S and summarized in Figure 1, the hydrolysis reaction rate (on a per gram basis of grafted glucan) on the surface of alumina in material AGL is 9-fold faster on a per glucan basis than the highest rate at 368 K measured on the silica surface, in material SGH. This effect cannot be explained by the increase in grafted active site density, as controlled by the density of OH-defect sites that are present during grafting, for material AGL relative to SGH, since the latter increase would only be expected to lead to approximately 3.3-fold increase in rate for AGL. This latter increase is represented by the extrapolated value for grafted β-glu strands on alumina, which is shown in Figure 1.

The significantly higher rate of grafted glucan hydrolysis observed for AGL relative to the extrapolation in Figure 1 requires a change in the nature of the active site for alumina relative to silica, and provides a unique perspective on attributes of a surface active site, for catalyzing glucan hydrolysis. Further confirmation regarding such a change in the nature of the active site for alumina versus silica is obtained by measuring the activation energy on both materials, since activation energy depends on the nature but not the density of active sites. We thus performed hydrolytic reactions for both AGL and SGH at a range of temperatures and summarize results in Table 2.

Hydrolysis rates of grafted β-glu strands in materials AGL and SGH within the temperature range 358−388 K are summarized in the Arrhenius plot of Figure 4 (see Figure 4S and Figure 5S of SI for raw rate data). The measured activation energies are 87 kJ/mol for silica support (material SGH) and 70 kJ/mol for alumina support (material AGL). The observed activation energy measured for the hydrolysis of the glycosidic bond in our materials is lower by 46 kJ/mol for SGH and 63 kJ/mol for AGL , when compared with acid-catalyzed reaction in dilute H_2SO_4, which has an activation energy of 133−138 kJ/mol.[23,24] Further comparing the measured reaction barriers to activation energies for β-glu hydrolysis using other systems (such as sulfonated carbon 110 kJ/mol[25] and cellulases 37−52 kJ/mol[26,27]) demonstrates a decrease in activation energy in the order of H_2SO_4 > sulfonated carbon > SGH > AGL > cellulase enzyme. The activation energy of sulfonated carbon material is slightly lower compared with that of homogeneous sulfuric acid, and this may be related to an apparent activation energy for the latter that incorporates a negative enthalpy of glucan adsorption (vide infra for discussion of glucan adsorption on carbon). It is interesting that the activation energy achieved with SGH and AGL, which both employ hydrogen bonds using weak acid sites, is actually lower than that measured previously for strong acid sites consisting of sulfonic and sulfuric acids.

The activation energy comparison above reflects a change in the nature of the active site for adsorbed glucan hydrolysis, between silica and alumina surfaces. Further insight into nature of the active site for adsorbed glucan hydrolysis and how this nature is affected by the OH-defect site density during aqueous reaction conditions can be obtained from data in Figure 5.

dx.doi.org/10.1021/ja311918z | J. Am. Chem. Soc. 2013, 135, 4398−4402

Table 1. Material Properties and Initial Rates of Reaction

sample	available grating sites [OH/nm^2]	BET surface area [m^2/g$_{support}$]	mass loss of β-glucan [mg/g$_{support}$][a,b]	initial hydrolysis rate at 95 °C [μmol h^{-1} g$^{-1}_{glucan}$]
AGL	14.2	100 ± 5	16 ± 3; (0.22 ± 0.2)	34.1 ± 2
SGH[c]	4.6	178 ± 5	51 ± 3; (0.43 ± 0.2)	3.8 ± 0.2
SGL[d]	2.0	193 ± 5	57 ± 3; (0.44 ± 0.2)	2.5 ± 0.2
SGEXL[d]	0.2	124 ± 5	37 ± 3; (0.44 ± 0.2)	0.6 ± 0.2

[a]Measured using TGA. [b]Values in parentheses represents the nondimensional packing density. [c]Physical properties of material are taken from ref 16. The initial rate is measured in Figure 2S (SI). [d]Data adapted from ref 16.

Table 2. Initial Hydrolysis Rates for SGH and AGL in a pH 4 Aqueous Solution at Various Temperatures

temperature [K]	SGH rate [μmol/h/g$_{glucan}$]	AGL rate [μmol/h/g$_{glucan}$]
358	–	25.8
368	3.8	34.1
378	10.0	66.1
388	16.1	158.1
activation energy [kJ/mol]	**87 ± 16**	**70 ± 12**

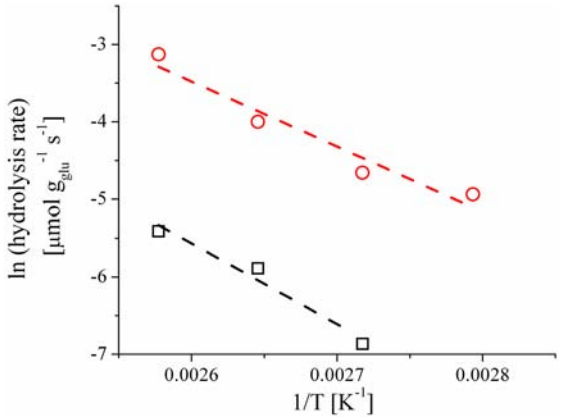

Figure 4. Arrhenius plot of the rate of β-glu hydrolysis in pH 4 aqueous solution. (○, red) AGL and (□) SGH. Dashed lines represent best fits via linear regression.

These data demonstrate that the rate of hydrolysis per grafted active site within all silica and alumina materials (the slope of dashed trend line in Figure 1 was used to represent all silica-based materials using the filled triangle symbol in Figure 5) increases linearly with density of OH-defect sites during hydrolysis catalysis. It is generally accepted that the mechanism of acid-catalyzed hydrolysis of the glycosidic bond follows a stepwise reaction mechanism where the rate-determining step is the formation of the half-chair oxocarbenium transition state from the ground-state chair conformation.[28]

Our data quantitatively measure the increase of surface-catalyzed hydrolysis rate and reduction of the hydrolysis activation barrier due to increasing concentration of surrounding OH-defect sites under aqueous reaction conditions. These data suggest that the rate-limiting step for hydrolysis is controlled by the probability of forming a hydrogen bond between the β-glu strand and the juxtaposed OH-defect sites on the surface. Our results further show that inducing rigid juxtapositioning of OH-defect sites of an inorganic-oxide surface as hydrogen-bond donors next to glycosidic oxygens of adsorbed β-glu strands activates the latter for hydrolysis (i.e., hydrolysis rate in AGL vs that in SGH).

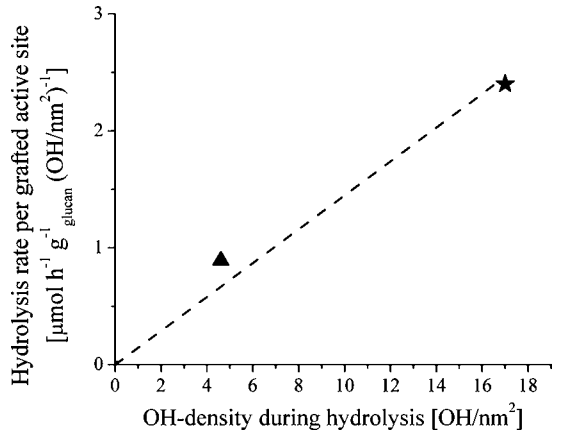

Figure 5. Rate of grafted β-glu strand hydrolysis normalized to grafted active-site surface density as a function of OH-defect site density during reaction. Reaction conducted in aqueous solution at 95 °C and pH 4: (▲) grafted β-glu strands on silica (representing grafted β-glu on silica materials SGEXL, SGL, and SGH using equation of linear regression trend line in Figure 1) and (★) grafted β-glu strands on alumina as represented by material AGL. Dashed line represents best-fit linear regression trend line.

The results above can be used to elucidate trends in emerging data when using unfunctionalized mesoporous carbon as a practical catalyst for cellulose hydrolysis. This catalyst, which consists of only weak-acid sites (i.e., sites limited to phenolic and carboxylic-acid OH groups[1,3,4]) was shown to demonstrate hydrolysis activity under mild conditions.[1,3,4] These results are intriguing insofar as the same hydrolysis reaction conducted in the presence of similarly acidic surfaces such as alumina demonstrate only a background level of hydrolysis activity.[3] We have recently demonstrated the adsorption of long-chain glucans into confining internal mesopores, which have a radius smaller than the calculated glucan radius of gyration (R_g).[2] On the basis of the results of Israelachvili et al. and Klein et al., who both demonstrated that the force needed to confine a polymer between two parallel plates increases exponentially as the distance between the walls approaches the polymer R_g,[29,30] we expect that the confined mesopore environment leads to highly constrained adsorbed glucan strands. We infer that these highly constrained glucans are forced to interact with OH-defect sites on the carbon surface, much like the grafted glucans in materials AGL and SGH above are constrained to interact with underlying OH-defect sites of the inorganic-oxide surface, due to adsorption. In the latter case, the ability to constrain a β-glu strand is enabled by the covalent M−O−glucan bonds (M = Al or Si) coupled with the known unfavorable aqueous-phase solubility of such long-chain glucans. In the former case, this constraint is enforced by many concerted weak CH−π interactions and hydrophobic interactions, which cause glucan adsorption within

dx.doi.org/10.1021/ja311918z | J. Am. Chem. Soc. 2013, 135, 4398−4402

the confining carbon mesopores, and significant mechanical strain on the bonds comprising the β-glu strand (*vide supra*). The latter mechanical strain is expected to facilitate hydrolysis as well, since hydrolysis relieves some of this strain via bond breaking. Mechanical strain is commonly invoked in hydrolytic enzyme mechanisms.[8,9] In all cases, the imposed constraining of the adsorbed β-glu strand enables close interaction of the glycosidic oxygens with juxtaposed OH-defect sites at high local concentrations, within the immediate vicinity of this strand. The data in this manuscript unequivocally demonstrate the importance of this juxtapositioning in the surface activation of the constrained β-glu strands for hydrolysis.

■ CONCLUSIONS

The results above demonstrate hydrolysis of constrained β-glu strands using a weak Brønsted acidic surface as catalyst. A high, local OH-defect site density on such a surface acts as an array of mild acidic sites to enforce a high probability of interaction between glycosidic oxygens and hydrogen-bond donors on the underlying surface. These results quantitatively elucidate essential features of weak Brønsted acid catalysts for cellulose depolymerization, such as unfunctionalized mesoporous carbon consisting of aromatic/aliphatic OH-defect sites. These features are (i) adsorption of the β-glu strand within a highly constrained environment that favors hydrogen bonding with OH-defect sites on the surface and (ii) an increasing probability of aforementioned hydrogen bonding, which activates glycosidic bonding for hydrolysis via the high, local density of OH-defect site donors during hydrolysis catalysis.

■ ASSOCIATED CONTENT

Supporting Information

Full synthesis protocol, Figures 1S−5S. This material is available free of charge via the Internet at http://pubs.acs.org.

■ AUTHOR INFORMATION

Corresponding Author

askatz@uclink.berkeley.edu

Notes

The authors declare no competing financial interest.

■ ACKNOWLEDGMENTS

The authors are grateful to the National Science Foundation for funding of this research (CBET 0854560). The authors acknowledge helpful technical discussions with Dr. John Roper III and Dr. James Bohling from The Dow Chemical Company.

■ REFERENCES

(1) Kobayashi, H.; Ohta, H.; Fukuoka, A. *Catal. Sci. Technol.* **2012**, *2*, 869.
(2) Chung, P.-W.; Charmot, A.; Gazit, O. M.; Katz, A. *Langmuir* **2012**, *28*, 15222.
(3) Kobayashi, H.; Komanoya, T.; Hara, K.; Fukuoka, A. *ChemSusChem* **2010**, *3*, 440.
(4) Kobayashi, H.; Yabushita, M.; Komanoya, T.; Hara, K.; Fujita, I.; Fukuoka, A. *ACS Catal.* **2013**, DOI: 10.1021/cs300845f.
(5) Saharay, M.; Guo, H.; Smith, J. C. *PLoS ONE* **2010**, *5*, e12947.
(6) Gazit, O. M.; Charmot, A.; Katz, A. *Chem. Commun.* **2011**, *47*, 376.
(7) Petersen, L.; Ardèvol, A.; Rovira, C.; Reilly, P. J. *J. Phys. Chem. B* **2009**, *113*, 7331.
(8) Atkinson, R. F.; Bruice, T. C. *J. Am. Chem. Soc.* **1974**, *96*, 819.
(9) Smith, B. J. *J. Am. Chem. Soc.* **1997**, *119*, 2699.
(10) Capon, B. *Tetrahedron Lett.* **1963**, *14*, 911.
(11) Storm, D. R.; Koshland, D. E. *Proc. Natl. Acad. Sci. U.S.A.* **1970**, *66*, 445.
(12) Kirby, A. J. In *Advances in Physical Organic Chemistry*; Bethell, D., Ed.; Academic Press: New York, 1994; Vol.*29*, p 87.
(13) Capon, B. *Chem. Rev.* **1969**, *69*, 407.
(14) Martinez, R.; Huff, M. C.; Barteau, M. A. *Appl.Catal., A* **2000**, *200*, 79.
(15) Heitmann, G. P.; Dahlhoff, G.; Hölderich, W. F. *J. Catal.* **1999**, *186*, 12.
(16) Gazit, O. M.; Katz, A. *Langmuir* **2012**, *28*, 431.
(17) Zhuravlev, L. T. *Colloids Surf., A* **2000**, *173*, 1.
(18) McHale, J. M.; Navrotsky, A.; Perrotta, A. J. *J. Phys. Chem. B* **1997**, *101*, 603.
(19) Lodziana, Z.; Norskov, J. K.; Stoltze, P. *J. Chem. Phys.* **2003**, *118*, 11179.
(20) O'Shaughnessy, B.; Vavylonis, D. *Eur. Phys. J. E: Soft Matter Biol. Phys.* **2003**, *11*, 213.
(21) Wang, J.-S.; Pandey, R. B. *Phys. Rev. Lett.* **1996**, *77*, 1773.
(22) Isogai, A.; Usuda, M.; Kato, T.; Uryu, T.; Atalla, R. H. *Macromolecules* **1989**, *22*, 3168.
(23) Liang, X.; Montoya, A.; Haynes, B. S. *J. Phys. Chem. B* **2011**, *115*, 10682.
(24) Bobleter, O.; Schwald, W.; Concin, R.; Binder, H. *J. Carbohydr. Chem.* **1986**, *5*, 387.
(25) Suganuma, S.; Nakajima, K.; Kitano, M.; Yamaguchi, D.; Kato, H.; Hayashi, S.; Hara, M. *J. Am. Chem. Soc.* **2008**, *130*, 12787.
(26) Hu, G.; Heitmann, J. A.; Rojas, O. J. *J. Phys. Chem. B* **2009**, *113*, 14761.
(27) He, D.; Bao, L.; Long, Y.; Wei, W.; Yao, S. *Talanta* **2000**, *50*, 1267.
(28) Moiseev, Y. V.; Khalturinskii, N. A.; Zaikov, G. E. *Carbohydr. Res.* **1976**, *51*, 23.
(29) Klein, J. *Nature* **1980**, *288*, 248.
(30) Horn, R. G.; Israelachvili, J. N. *Macromolecules* **1988**, *21*, 2836.